arXiv:1407.0802v2 [cond-mat.mes-hall] 26 Nov 2014

Origin of the Phonon Hall Effect in Rare-Earth Garnets

Michiyasu Mori,[1] Alexander Spencer-Smith,[2] Oleg P. Sushkov,[3] and Sadamichi Maekawa[1]

[1]*Advanced Science Research Center, Japan Atomic Energy Agency,Tokai 319-1195, Japan*
[2]*School of Physics, University of Sydney, Sydney 2006, Australia*
[3]*School of Physics, University of New South Wales, Sydney 2052, Australia*

(Dated: November 27, 2014)

The phonon Hall effect has been observed in the paramagnetic insulator, $Tb_3Gd_5O_{12}$. A magnetic field applied perpendicularly to a heat current induces a temperature gradient that is perpendicular to both the field and the current. We show that this effect is due to resonant skew scattering of phonons from the crystal field states of superstoichiometric Tb^{3+} ions. This scattering originates from the coupling between the quadrupole moment of Tb^{3+} ions and the lattice strain. The estimated magnitude of the effect is consistent with experimental observations at $T \sim 5$ K, and can be significantly enhanced by increasing temperature.

PACS numbers: 66.70.-f, 72.20.Pa, 72.15.Gd

When a linear magnetic field is applied perpendicularly to a heat current in a sample of terbium gallium garnet (TGG), $Tb_3Ga_5O_{12}$, a transverse temperature gradient is induced in the third perpendicular direction[1,2]. This is the "phonon Hall effect (PHE)". The effect was observed in this insulator at low temperature ($T \sim 5$ K), a situation in which there are no mobile charges such as electrons or holes[3]. The Neel temperature of TGG is 0.24 K[4], so it is a paramagnet at $T \sim 5$ K. Hence magnons do not contribute to the heat current and one does not expect a contribution from the magnon Hall effect[5–8]. Phonons are not charged and hence cannot be affected by the Lorentz force which gives rise to the usual classical Hall effect. Therefore the mechanism for the PHE must be related to the spin-orbit interaction. However, the spin-orbit interaction for phonons is not at all obvious, unlike in the anomalous Hall effect and spin Hall effect for electrons[9–11]. Thus, an understanding of the origin of the observed PHE is a fundamental problem.

So far, there have been a few theoretical attempts to explain the PHE[12–15]. Refs. 12 and 13 assumed a Raman-type interaction between the spin of stoichiometric Tb^{3+} ions and the phonon. This interaction results in "elliptically polarized" phonons. According to 12,13, the "elliptic polarization", in combination with scattering from impurities, leads to the PHE. In this scenario the type of impurity is unimportant and hence phonon – impurity scattering is considered in the leading Born approximation. This is an intrinsic-extrinsic scenario, i.e., the "elliptic polarization" is an intrinsic effect and the scattering from impurities is an extrinsic effect. The major problem with this scenario was realized in Ref. 14 - in spite of the "elliptic polarization" the Born approximation does not result in the PHE. Ref. 14 attempted to go beyond the leading Born approximation in impurity scattering. However, the problem has not been resolved yet. An intrinsic mechanism for the PHE, based on the Berry curvature of phonon bands, was suggested in Ref. 15. This is similar to the Berry curvature mechanism in the Hall effect for light[16]. The Berry curvature mechanism is certainly valid for materials with specially structured phonon bands, however, it is hard to see how the mechanism can be realized in TGG which has the simple cubic structure.

There is an important experimental observation which was missed in all the previous theoretical analyses of the PHE - TGG crystals can be grown by the flux method (TGG_{fl}), and by the Czochralski method (TGG_G). While TGG_{fl} has perfect stoichiometry, TGG_G contains about 1% of superstoichiometric Tb^{3+} ions. At 5 K the diagonal thermal conductivity of TGG_G is about 5 times smaller than that of TGG_{fl}[17]. This indicates that the thermal conductivity in TGG_G is determined by phonon scattering from the crystal field states of superstoichiometric Tb^{3+} ions[17]. The PHE has only been observed in TGG_G[1,2]. Thus, one concludes that the PHE is of extrinsic origin - due to the phonon scattering from superstoichiometric Tb^{3+} ions. We stress that the PHE in TGG relies specifically upon scattering from superstoichiometric Tb^{3+} ions, not just scattering from any impurities. This observation was not considered in all previous suggestions[12,13,15] for the mechanism behind the PHE.

In this Letter, motivated by the above observation, we show that the PHE originates from the resonant skew scattering of phonons from the crystal field states of superstoichiometric Tb^{3+} ions. Below, we will often refer to superstoichiometric Tb^{3+} ions as impurities.

Phonons.– The phonon Lagrangian density reads

$$\mathcal{L}_0 = \frac{\rho}{2}\left\{\dot{\varphi}_j^2 - c_T^2(\partial_i\varphi_j)^2 - (c_L^2-c_T^2)(\partial_i\varphi_i)(\partial_j\varphi_j)\right\},$$
$$\boldsymbol{\varphi} = \sum_{\boldsymbol{q},\mu}\frac{\boldsymbol{e}_\mu}{\sqrt{2\rho\omega_{\boldsymbol{q}\mu}}}\left[a_{\boldsymbol{q}\mu}e^{-i\omega_{\boldsymbol{q}\mu}t+i\boldsymbol{q}\cdot\boldsymbol{r}} + h.c.\right]. \quad (1)$$

Here $\boldsymbol{\varphi}$ is lattice displacement. The isotropic model (1) is known to be appropriate for a system with a large unit cell, such as that of a garnet[20–22]. The index $\mu = 1, 2, 3$ enumerates phonon polarization, $\boldsymbol{e}^{(\mu)}$ is the unit polarization vector, $a_{\boldsymbol{q}\mu}$ is the annihilation operator of the phonon, and $\omega_{\boldsymbol{q}\mu} = c_L q$ ($c_T q$) is the energy of the longitudinal (transverse) phonon. For the purpose of making estimates, we will use the following value of speed: $c \approx 3.7 \times 10^5$ cm/s, and the mass density: $\rho = 7.2$

g/cm^3[17]. Below, only the longitudinal mode is considered. It is plausible that this mode dominates PHE due to its large velocity, $c_L \approx 2c_T$[21]. Even if transverse modes gave comparable contribution, this does not influence our estimate of the effect.

Tb ion.– The $^7F_6$ state of a free Tb^{3+} ion splits into 13 levels in the dodecahedral crystal field of the garnet. The energies of low lying levels in intrinsic ions are approximately 0, 3, 49, 62, 72, 76 K[23,24]. The energy levels of impurity ions (superstoichiometric) depend on their particular positions, but overall they are comparable to those of ions in regular sites. The thermal conductivity in TGG_G is mainly determined by the resonant scattering of phonons from superstoichiometric ions. Note that resonant scattering necessarily implies a nonzero scattering phase and hence gives rise to skew scattering, which does not appear in the Born approximation[25].

Fitting the measured diagonal thermal conductivity[17] within four levels of the impurity ion, we come to the ion level scheme shown in Fig. 4 left, $\omega_{ab} = 3$K, $\omega_{ac} = 20$K, $\omega_{ad} = 70$K (see supplemental material). It is known that the ground state energy doublet is very sensitive to magnetic field B. At $T = 4.2$K and $B < 1$T the ion magnetic moment grows linearly with B. At fields larger than 1-2 T, the magnetic moment practically saturates at $|M| \approx 4\ \mu_B$[26]. This data indicates that the a,b-states are composed of time conjugate states $|\pm M\rangle$, $|a\rangle \propto |+M\rangle + |-M\rangle$, $|b\rangle \propto |+M\rangle - |-M\rangle$, and, subjected to a under magnetic field, the a,b-states evolve to $|\pm M\rangle$ as shown in Fig. 4 right, $\omega_{ab} \to \Omega_{a'b'} = \sqrt{\omega_{ab}^2 + (2gB)^2}$ with an effective g factor[27]. Below, we assume that, for

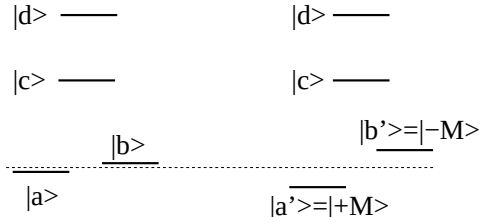

FIG. 1: The crystal field levels for $B = 0$ on the left, and for $B > 1 - 2$ T on the right.

the magnetic field larger than 1-2 T, only the state $|a'\rangle = |+M\rangle$ is thermally populated, while, without magnetic field, both $|a\rangle$ and $|b\rangle$ are populated. For simplicity we assume that $|c\rangle$ and $|d\rangle$ are not sensitive to the magnetic field.

Spin-phonon interaction.– The quadrupole Coulomb interaction of a Tb ion with its surrounding lattice ions is of the following form[18,19],

$$H_1 = \gamma T_{ij}\partial_i\varphi_j \qquad (2)$$
$$T_{ij} = \frac{3}{2J(2J-1)}\left\{J_iJ_j + J_jJ_i - \frac{2}{3}J(J+1)\delta_{ij}\right\} .$$

Here φ_j is the lattice displacement at the ion site $i, j = x, y, z$. The quadrupole moment $Q_{ij} = QT_{ij}$ is written in terms of the total angular momentum J. This implies that the strong spin orbit interaction inside the ion core is embedded in Eq. (2). The size of an ion core is about one Bohr radius a_B. Hence, the quadrupole moment Q is roughly estimated as $Q \sim ea_B^2$, where e is the elementary charge. The gradient of the electric field E from the surrounding ions is estimated as $\nabla E \sim e/d^3$, where $d \approx 2\mathring{A}$ is the distance to the nearest oxygen ion. Then, the magnitude of the coupling γ is,

$$\gamma \sim Q\nabla E \sim \frac{e^2a_B^2}{d^3} \sim 0.7 \text{ eV} . \qquad (3)$$

Resonant scattering.– Phonon scattering from superstoichiometric Tb^{3+} ions is determined by the diagram in Fig. 5. Under nonzero magnetic field, a straightforward calculation gives the following scattering rate for a phonon with energy ω,

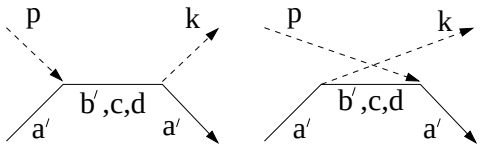

FIG. 2: Amplitude of phonon scattering from a Tb ion with virtual excitation of the crystal field level given magnetic field larger than 1-2 T. The solid line shows the ionic state and the dashed-line shows the phonon. Without the magnetic field, the initial state a' is substituted by the states a or b, with c and d as intermediate states.

$$\tau_\omega^{-1} = \tau_L^{-1} + \sum_{i=b',c,d}\tau_{a'i,\omega}^{-1},$$
$$\tau_{a'i,\omega}^{-1} = \frac{N_s}{N_{Tb}}\frac{\omega_D^3\omega^4}{80\pi}\frac{(\Omega_{a'i}/\omega_{ai})^2\Gamma_{ai}^2/\omega_{ai}^4}{(\omega^2-\Omega_{a'i}^2)^2+\Omega_{a'i}^2\Gamma_{i\omega}^2},$$
$$\Gamma_{ai} = \gamma^2\omega_{ai}^3/\pi\rho c^5 , \quad \Gamma_{i\omega} = (\omega/\omega_{ai})^3\Gamma_{ai} \qquad (4)$$

Here $\tau_L^{-1} = c/L$ is due to the finite size of the sample $L \approx 1$mm. The total density of Tb ions is $N_{Tb} \approx 1.3 \times 10^{22}$cm^{-3}, the density of superstoichiometric Tb ions is $N_s \approx 1.5 \times 10^{20}$cm^{-3}, and the Debye frequency/temperature is $\omega_D = 487$ K[17]. Eq. (4) is similar to that derived a long time ago in Refs. 28,29. It is worth noting that the ω^4 dependence in the numerator of the resonant part of τ_ω^{-1} originates from the derivative in the interaction (2). This derivative is enforced by Adler's theorem[30].

Skew component.– We take the magnetic field directed along the z-axis. The phonon propagates in the xy-plane with an initial momentum $\boldsymbol{k} = k(1, 0, 0)$ and final momentum $\boldsymbol{q} = k(\cos\phi, \sin\phi, 0)$, where ϕ is the scattering angle. When the magnetic field is small, the states a' and b' are populated and then the diagrams in Fig. 5 give the following phonon angular distributions for scattering (see Ref. 31 and supplemental material),

$$W_{\boldsymbol{k}\to\boldsymbol{q}}^{a'c} \approx \frac{\tau_{a'c,\omega}^{-1}}{2\pi}\left(\cos^2\phi - \frac{\omega\Gamma_{c\omega}}{\Omega_{a'c}^2}\cos\phi\sin\phi\right) , \qquad (5)$$

$$W^{b'c}_{\boldsymbol{k}\to\boldsymbol{q}} \approx \frac{\tau^{-1}_{b'c,\omega}}{2\pi}\left(\cos^2\phi + \frac{\omega\Gamma_{c\omega}}{\Omega^2_{b'c}}\cos\phi\sin\phi\right). \quad (6)$$

Note that the second term proportional to $\sin\phi$ is the skew component and the sign of the $a'c$ process is opposite to that of the $b'c$ process. This is due to the time-conjugation of the states $|a'\rangle = |+M\rangle$ and $|b'\rangle = |-M\rangle$. Without the magnetic field, these process cancel each other out, whereas with a magnetic field the skew component becomes finite for two reasons - the energy difference between $\Omega_{a'c}$ and $\Omega_{b'c}$, and the de-population of the state b'. The $a'b'$ and $b'a'$ processes also contribute to scattering such as Eqs. (20) and (6), respectively. If the states a' and b' are equally populated, the skew components in these processes cancel each other out, since $\tau_{a'b',\omega} = \tau_{b'a',\omega}$ and $|\Omega_{b'a'}| = |\Omega_{a'b'}|$. When the state b' is depopulated by increasing the magnetic field, the cancellation becomes imperfect and the $a'b'$ process also contributes to the skew scattering.

Correlation of impurity positions.– The $\cos\phi\sin\phi$ term in Eqs. (20) and (6) change sign at $\phi\to-\phi$. This is the skew asymmetry which is necessary for the PHE. However, this term also changes sign at $\phi\to\pi-\phi$. Because of this, the off-diagonal thermal conductivity is zero, $\kappa_{xy}=0$, in spite of the skew since skew scattering in the forward hemisphere, $\cos\phi>0$, is exactly compensated for by skew scattering in the backward hemisphere, $\cos\phi<0$. There is no such problem for electron skew scattering[32], but there is a similar problem for the skew scattering of light. There are two mechanisms which destroy the $\phi\to\pi-\phi$ compensation: (i) Spatial correlation of impurity positions discussed below; (ii) Interference between contributions with different values of ΔJ_z, this mechanism is discussed in the supplemental material.

A superstoichiometric Tb^{3+} ion has ionic radius 0.92Å and it replaces a Ga^{3+} ion with smaller radius 0.62Å. Hence the crystal lattice around the Tb ion is elastically deformed towards larger lattice spacing. During the process of crystal growth this creates more room for another superstoichiometric Tb ion in the vicinity of the first one. Hence the impurity density $\rho_s(\boldsymbol{r})$ must be correlated as

$$\overline{\rho_s(0)\rho_s(\boldsymbol{r})} = N_s\delta(\boldsymbol{r}) + N_s^2[1+Ce^{-r/l}], \quad (7)$$

where the correlation length is about the average distance between impurities, $l\approx N_s^{-1/3}\approx 2\times10^{-7}$ cm. Given the significant difference in ionic radii it is natural to assume about a 50% change in the probability of having another superstoichiometric Tb ion in the vicinity of the first one. Hence, it is reasonable to expect that the correlation constant is $C\sim\pm1$. Due to the correlation (7), the interference between phonon scattering amplitudes from adjacent impurities is nonzero and the scattering probability Eq. (20) is modified by an interference term as: $W_{k\to q}\to W_{k\to q}(1+CP_\phi)$, where $P_\phi = 1/[1+(2kl\sin\phi/2)^2]^2$. Thus, the correlation destroys the $\phi\to\pi-\phi$ compensation factor. It is convenient to expand P_ϕ in series of Legendre polynomials $P_\phi = a_0(\omega) + a_1(\omega)P_1(cos\phi) + ...$, where

$$a_1(\omega) = \frac{3}{(\omega/\omega_1)^2}\left[1+\frac{1}{1+(\omega/\omega_1)^2}\right] - \frac{6}{(\omega/\omega_1)^4}\ln\left[1+(\omega/\omega_1)^2\right], \quad (8)$$

and $\omega_1\equiv\hbar c/2l\approx 13$K. Hence, accounting for the mechanisms (i) (see also supplemental material), the scattering rate given by Eqs. (20) and (6) is transformed to

$$W_{\boldsymbol{k}\to\boldsymbol{q}} \approx \frac{\tau^{-1}_\omega}{4\pi}\left\{1-\mathcal{K}_\omega\omega\Gamma_{c\omega}\boldsymbol{n}_B\cdot[\boldsymbol{n}_k\times\boldsymbol{n}_q]\right\}, \quad (9)$$

$$\mathcal{K}_\omega = \frac{C}{5}a_1(\omega)\tau_\omega\left(\frac{\tau^{-1}_{a'c,\omega}}{\Omega^2_{a'c}} - n_T\frac{\tau^{-1}_{b'c,\omega}}{\Omega^2_{b'c}} + \bar{n}_T\frac{\tau^{-1}_{a'b',\omega}}{\Omega^2_{a'b'}}\right),$$

$$n_T\equiv\exp[-\Omega_{a'b'}/T]\equiv 1-\bar{n}_T,$$

where $\boldsymbol{n}_B,\boldsymbol{n}_k,\boldsymbol{n}_q$ are unit vectors along the direction of the magnetic field and the phonon momenta respectively, and n_T and $\bar{n}_T$ are the thermal populations.

Phonon Hall effect. – The Boltzmann equation for the phonon distribution function, $f_k = f_k^{(0)} + g_k^{(S)} + g_k^{(A)}$, reads[33],

$$c^2\mathbf{k}\cdot\left(\frac{\nabla T}{T}\right)\left(-\frac{\partial f^{(0)}_{\boldsymbol{k}}}{\partial\omega_k}\right) \approx \sum_q (W_{\boldsymbol{q}\to\boldsymbol{k}}f_{\boldsymbol{q}} - W_{\boldsymbol{k}\to\boldsymbol{q}}f_{\boldsymbol{k}}). \quad (10)$$

Here $f_k^{(0)}$ is the equilibrium Bose-Einstein distribution. Since the scattering rate (21) contains both the symmetric part, $W^{(S)}_{q\to k} = W^{(S)}_{k\to q}$ and the asymmetric part, $W^{(A)}_{q\to k} = -W^{(A)}_{k\to q}$, we need to account for the two non-equilibrium components, $g_k^{(S)}$ and $g_k^{(A)}$,

$$g_k^{(S)}\propto(\boldsymbol{k}\cdot\boldsymbol{\nabla}T)\,, \quad g_k^{(A)}\propto(\boldsymbol{k}\cdot[\boldsymbol{n}_B\times\boldsymbol{\nabla}T]). \quad (11)$$

Assuming that the asymmetry parameter in Eq. (21) is small, $\mathcal{K}_\omega\omega\Gamma_{c\omega}\ll 1$, solution of the Boltzmann equation is straightforward and results in the following non-equilibrium part of the distribution function,

$$g_k^{(S)} + g_k^{(A)} = -\frac{e^{\omega_k/T}}{(e^{\omega_k/T}-1)^2}\frac{c^2}{T^2}\tau_\omega \times\left\{(\boldsymbol{k}\cdot\boldsymbol{\nabla}T) - \frac{1}{3}\mathcal{K}_\omega\omega\Gamma_\omega(\boldsymbol{k}\cdot[\boldsymbol{n}_B\times\boldsymbol{\nabla}T])\right\}. \quad (12)$$

Hence, we calculate the diagonal- and the off-diagonal thermal conductivities as,

$$\kappa_{xx} = \frac{T^3}{2\pi^2c}\int\tau_\omega\frac{x^4e^xdx}{(e^x-1)^2}, \quad (13)$$

$$\kappa_{xy} = \frac{T^3}{2\pi^2c}\int\tau_\omega\frac{\mathcal{K}_\omega}{3}\omega\Gamma_\omega\frac{x^4e^xdx}{(e^x-1)^2}, \quad (14)$$

where $x\equiv\omega/T$. The diagonal thermal conductivity in Eq. (13) is of the standard form[34], which is used to fit

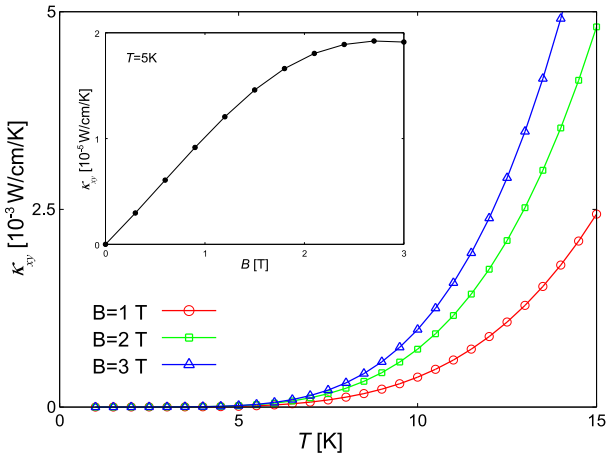

FIG. 3: Magnetic field dependence of the transverse component of thermal conductivity κ_{xy} [10^{-3}W/cm/K]. Inset is the magnetic field dependence of κ_{xy} [10^{-5}W/cm/K] at $T = 5$ K. Here, $g = 1$ and $\omega_{ab} = 0$ and the state d is ignored.

the data in Ref. 17. The transverse thermal conductivity κ_{xy} given by Eq. (14) is shown in Fig. 3 as a function of T with B=1,2,3 T. We can see that κ_{xy} is enhanced by T and B (See also the inset in Fig. 3). Note that this results is justified for $T < \Omega_{a'c} \sim$20 K, since the state c is assumed to be un-populated. The inset in Fig. 3 is the B-dependence of κ_{xy}, which increases and finally starts to decrease around $B \sim$2.5 T.

Our estimate of the phonon Hall angle, S, immediately follows from Eqs. (13) and (14) and, for magnetic field larger than 1-2T, is,

$$S \equiv \frac{1}{B}\frac{\kappa_{xy}}{\kappa_{xx}} \tag{15}$$

Assuming that at temperature $T = 5$K the frequency is $\omega = T = 5$K, Eq. (15) results in the following estimate: $S(T = 5K) \sim 5 \cdot 10^{-4}$rad/T. An accurate evaluation of the integrals in Eq.(13) confirms that the primary contribution to κ_{xx} comes from $\omega \approx T = 5$K. On the other hand the dominant contribution to κ_{xy} comes from $\omega \sim 30$K - the phonon Hall effect is due to relatively "hot" phonons. Accounting for the hot phonon effect enhances our theoretical estimate: $S(T = 5K) \sim 10^{-3}$rad/T. Our estimate is reasonably consistent with measurements, $S(T = 5.45K) \approx 1 \cdot 10^{-4}$rad/T[1] and $S(T = 5.13K) \approx 0.35 \cdot 10^{-4}$rad/T[2]. The presented theoretical estimates of κ_{xy} correspond to $C \sim 1$. Important is that C-dependence of the Hall angle may explain the significant difference between the two measurements, i.e., two different crystals were used in the two measurements[1,2] (see also supplemental material).

Conclusion.– We have shown that the puzzling phonon Hall effect observed in $Tb_3Gd_5O_{12}$, is due to the resonant skew scattering of phonons from the crystal field levels of superstoichiometric Tb^{3+} ions. The obtained magnitude of the effect is in agreement with experiments performed at $T = 5$ K. We predict that the magnitude of the effect grows very significantly with temperature in the interval 3 K $< T <$ 15 K. Compared to the performed measurements we expect the effect to be about an order of magnitude larger at $T = 10 - 15$ K. A mechanism similar to that considered here for the phonon Hall effect is also valid for the Hall effect of light[35]: skew scattering of light from atomic/molecular transitions. For light the quadrupole crystal field interaction Eq. (2) should be replaced by the electric dipole interaction.

Acknowledgments

We would like to thank A. I. Milstein, G. Khaliullin and G. Jackeli for stimulating discussions. This work was supported by the Grant-in-Aid for Scientific Research and bilateral program from MEXT. M.M. thanks the Godfrey Bequest and the School of Physics at the University of New South Wales for financial support and kind hospitality. O.P.S. thanks the Japan Society for Promotion of Science and Advanced Science Research Centre JAEA for financial support and kind hospitality.

SUPPLEMENTAL MATERIALS

I. RESONANT SCATTERING IN THERMAL CONDUCTIVITY

The thermal conductivity κ_{xx} of $Tb_3Gd_5O_{12}$ (TGG) has been studied by Inyushkin and Taldenkov who measured and analysed the conductivity[17]. They fit the temperature dependence of κ_{xx} by supposing four processes; boundary, point defect, umklapp, and resonant scatterings. It is concluded that *at helium temperatures for which the phonon Hall effect was detected, κ_{xx} is almost completely determined by resonance scattering from impurity ions and scattering from boundaries (size of the sample)*[17]. Following their results, we read the experimental data of Fig. 2 in Ref. 17 and plotted in Fig. 4 by circles (red). To obtain the minimal level scheme at $T <$ 15 K (See Fig. 1 in the main text), we use the following equations, which are equivalent to Eqs. (4) and (13) in the main text,

$$\kappa_{xx} = \frac{T^3}{2\pi^2 c}\int_0^{\omega_D/T} \tau_\omega \frac{x^4 e^x dx}{(e^x-1)^2}, \tag{16}$$

$$\tau_\omega^{-1} = \tau_L^{-1} + \sum_{i=,b,c,d} \tau_{ai,\omega}^{-1}, \tag{17}$$

$$\tau_{ai,\omega}^{-1} = \frac{N_s}{N_{Tb}}\frac{\omega_D^3\omega^4}{80\pi}\frac{(\Omega_{ai}/\omega_{ai})^2\Gamma_{ai}^2/\omega_{ai}^4}{(\omega^2-\Omega_{ai}^2)^2+\Omega_{ai}^2\Gamma_{i\omega}^2}, \tag{18}$$

$$\Gamma_{ai} = \frac{\gamma_i^2\omega_{ai}^3}{\pi\rho c^5} = \frac{\gamma_i^2\omega_{ai}^3}{\pi\omega_D^3(\rho c^2/40\pi^2 N_{Nb})}$$

$$\Gamma_{i\omega} = \left(\frac{\omega}{\omega_{aj}}\right)^3 \Gamma_{aij},$$

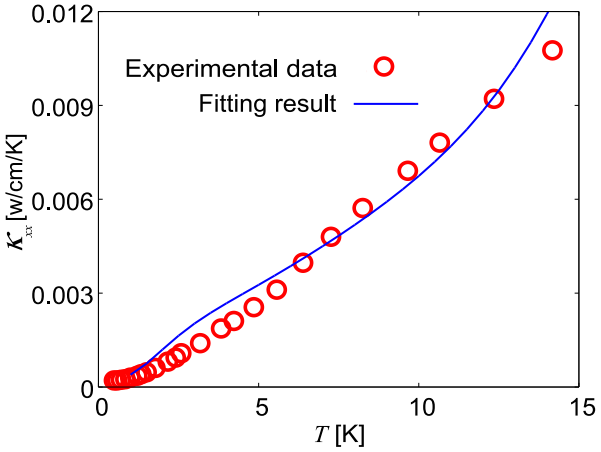

FIG. 4: The thermal conductivity due to the resonant scattering. The circles (red) are obtained by the experimental data (See Fig. 2 in Ref. 17) and the solid line (blue) is our fitting result by the minimal model (See Fig. 1 left in the main text).

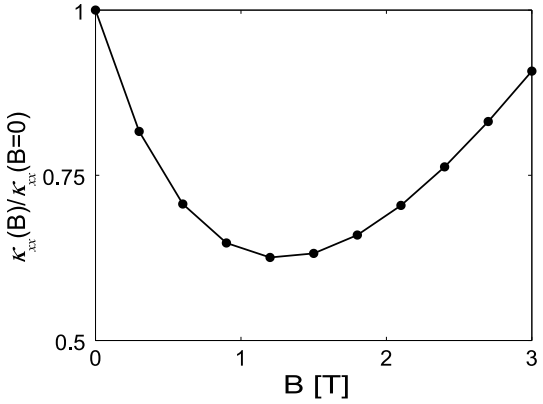

FIG. 5: Magnetic field dependence of $\kappa_{xx}(B)$ normalized by its magnitude without magnetic field $\kappa_{xx}(B=0)$.

where $x \equiv \omega/T$, $c = 3.72 \times 10^5$ cm/s, and the mass density $\rho = 7.2$ g/cm^3[17]. Here $\tau_L^{-1} = c/L$ is due to the finite size of the sample $L \approx 1$mm (boundary scattering). The total density of Tb ions is $N_{Tb} \approx 1.3 \times 10^{22}$cm^{-3}, the density of superstoichiometric Tb ions is $N_s \approx 1.5 \times 10^{20}$cm^{-3}, and the Debye temperature is $\omega_D = 487$ K[17]. Note that in the considered temperature range the upper limit of integration in Eq. (16) is $\omega_D/T > 30$, so we can safely set it equal to ∞. We found that to fit κ_{xx} in the temperature range $T < 15K$ one needs minimum four levels. Three lowest levels are determined from the fit quite accurately, $\omega_{ab} = 3$ K, $\omega_{ac} = 20$ K, $\omega_{bc} = 17$ K. The topmost level, which describes a cumulative effect of all higher states, is somewhat ambiguous, we take $\omega_{ad} = 70$ K, and $\omega_{bd} = 67$ K. The fit with $\gamma_{ab} = 1.5$ eV, $\gamma_{ac} = \gamma_{bc} = 0.6$ eV, $\gamma_{ad} = \gamma_{bd} = 0.8$ eV is shown in Fig.4 by blue solid line. The contribution of the topmost d-level is relatively small, but still it is important for the fit. This contribution scales as $\propto \gamma_{ad}^2/\omega_{ad}^2$, therefore one can always increase γ_{ad} and ω_{ad} proportionally. Note that since we do not account for thermal population of the c-level, our fit starts to deviate from experimental data at $T > 15K$.

II. MAGNETIC FIELD DEPENDENCE OF THERMAL CONDUCTIVITY

It is known that the ground state energy doublet is very sensitive to magnetic field B as shown in the right part of Fig. 1 in the main text, $\omega_{ab} \to \Omega_{a'b'} = \sqrt{\omega_{ab}^2 + (2gB)^2}$. The κ_{xx} in a magnetic field calculated at $T = 5$ K with values of parameters presented above is shown in Fig. 5. For simplicity we assume that $|c\rangle$ and $|d\rangle$ are not sensitive to the magnetic field. The suppression of κ_{xx} by a magnetic field is reported in Ref. 17, and our result is close to the data obtained by the magnetic field in the [111] direction. We find that the split of the quasi-doublet state is the main source of such a suppression. However, to fit the angle dependence of κ_{xx} from Ref. 17, one needs to account different crystallographic positions of superstoichiometric Tb ions with different orientations of crystal fields. In addition, a kind of magnetostriction would be involved in such a magnetic field dependence of κ_{xx}. In the present work we disregard these fine details.

III. SKEW SCATTERING PROBABILITY

We already pointed out, Ref. [27] in the main text, that $|\pm M\rangle$ states are composed of states with definite z-projection of the ion angular momentum J such as,

$$|+M\rangle = ...|+2\rangle + \alpha_+|+1\rangle + \alpha_0|0\rangle + \alpha_-|-1\rangle + ...$$
$$|-M\rangle = ...|-2\rangle - \alpha_+|-1\rangle + \alpha_0|0\rangle - \alpha_-|+1\rangle + ... \quad (19)$$

The structure of c- and d-states is similar. Matrix elements of the interaction Hamiltonian (2) come from transitions with $\Delta J_z = \pm 1$ and with $\Delta J_z = \pm 2$. It is easy to check that in the scattering amplitude Fig. 2 the contributions with $\Delta J_z = \pm 1$ result in $\cos\phi$ or $\sin\phi$ and the contributions with $\Delta J_z = \pm 2$ result in $\cos 2\phi$ or $\sin 2\phi$. Therefore, the scattering probability reads

$$W_{\boldsymbol{k}\to\boldsymbol{q}}^{a'c} \propto \left\{ A_1 \left[\cos\phi - \frac{\omega\Gamma_{c\omega}}{2\Omega_{a'c}^2} \sin\phi \right] + A_2 \left[\cos 2\phi - \frac{\omega\Gamma_{c\omega}}{2\Omega_{a'c}^2} \sin 2\phi \right] \right\}^2 , \quad (20)$$

In Eqs. (5) and (6) in the main text for simplicity we set $A_2 = 0$. Generally, while one expects some suppression of the second harmonic, $A_2/A_1 < 1$, the harmonic is of course nonzero. A particular value of A_2/A_1 depends on the coefficients in the wave functions (19). Both the A_1^2-term and the A_2^2-term in (20) have the $\phi \to \pi - \phi$ compensation problem. These terms, as it is described in the

main text, contribute to PHE only due to correlation of positions of impurities. This contribution is proportional to the correlation coefficient C in Eq.(9). We think that this is the leading term dominating the skew scattering and can explain the sample dependence of PHE. However, there is also the A_1A_2 interference term in (20). The interference term results in the forward-backward scattering asymmetry and hence the terms does not have the $\phi \to \pi - \phi$ compensation problem. This interference contribution in Eq.(9) is *not* proportional to the impurity correlation coefficient C. Hence, the skew scattering is always there, even if the impurity correlation C was ignored. The term proportional to $A_2/A_1 > 0$ implies that the forward phonon scattering dominates over the backward one, which is intuitively natural. In this study, we consider that the contribution of A_2/A_1-term will be smaller than that of C-term to the PHE. Detail analysis on the electronic states of TGG will judge this point in the future.

IV. DERIVATION OF EQ. (9) IN THE MAIN TEXT

In the main text we point out that there are two mechanisms which destroy $\phi \to \pi - \phi$ compensation: (i) Spatial correlation of impurity positions; (ii) Interference between contributions with different values of ΔJ_z. Here we show how the mechanism (i) works. Eq. (20) results in the following skew terms

$$W^{(1)}_{\boldsymbol{k}\to\boldsymbol{q}} \propto (\boldsymbol{n}_k \cdot \boldsymbol{n}_q)(\boldsymbol{n}_B \cdot [\boldsymbol{n}_k \times \boldsymbol{n}_q]) \tag{21}$$

$$W^{(2)}_{\boldsymbol{k}\to\boldsymbol{q}} \propto \frac{A_2}{A_1}(\boldsymbol{n}_B \cdot [\boldsymbol{n}_k \times \boldsymbol{n}_q]) \ . \tag{22}$$

Here we neglect small A_2^2 terms and A_2/A_1 term is discussed above. The multiplier $(\boldsymbol{n}_k \cdot \boldsymbol{n}_q)$ in $W^{(1)}$ leads to the $\phi \to \pi - \phi$ compensation in κ_{xy}. It is discussed in the main text that the spatial correlation of impurities transforms $W^{(1)}$ due to P_ϕ such as,

$$W^{(1)}_{\boldsymbol{k}\to\boldsymbol{q}} \ \to \ P_\phi W^{(1)}_{\boldsymbol{k}\to\boldsymbol{q}} \to C a_1(\omega)(\boldsymbol{n}_k \cdot \boldsymbol{n}_q)^2(\boldsymbol{n}_B \cdot [\boldsymbol{n}_k \times \boldsymbol{n}_q]) \ . \tag{23}$$

This expression does not contain the $\phi \to \pi - \phi$ compensation. Now we want to reduce (23) to the standard skew correlation $(\boldsymbol{n}_B \cdot [\boldsymbol{n}_k \times \boldsymbol{n}_q])$ used in Eq.(9) in the main text. A naive way is just to replace $(\boldsymbol{n}_k \cdot \boldsymbol{n}_q)^2 \to 1/2$. However, this is an obvious overestimation, the correlation $(\boldsymbol{n}_B \cdot [\boldsymbol{n}_k \times \boldsymbol{n}_q]) = \sin\phi$ is maximum at $\phi = \pi/2$ where $(\boldsymbol{n}_k \cdot \boldsymbol{n}_q)^2 = (\cos\phi)^2$ is zero. The correct way is to substitute (23) in Eq.(10), solve the kinetic equation with respect to $g_k^{(A)}$ defined in Eq.(11), and finally map the solution back to the simple skew correlation $(\boldsymbol{n}_B \cdot [\boldsymbol{n}_k \times \boldsymbol{n}_q])$. It is noted that most of term in Eq.(11) substituted by (23) and $g_k^{(A)}$ disappears due to the symmetry, e.g., $\int d\Omega_q g_q^{(A)} = 0$ and so on. The solution of kinetic equation contains averaging of the fourth rank tensor $\langle n_\alpha n_\beta n_\gamma n_\delta \rangle$, which gives the factor 1/5 (see also Eq. (26)). All in all, this procedure leads to the term $\frac{C}{5}a_1(\omega)$ in the square brackets in the second line of Eq. (9).

V. DERIVATION OF EQ. (12) IN THE MAIN TEXT

Quantities which enter in the r.h.s of Eq. (10) in the main text are of the following form

$$\begin{aligned} W_{\boldsymbol{k}\to\boldsymbol{q}} &= \frac{\tau_\omega^{-1}}{4\pi}\left\{1 - a \cdot \boldsymbol{n}_B \cdot [\boldsymbol{n}_k \times \boldsymbol{n}_q]\right\}, \qquad (24) \\ f_{\boldsymbol{k}} &= f^{(0)}_{\boldsymbol{k}} + A^S \boldsymbol{n}_{\boldsymbol{k}} \cdot \nabla T + A^A \boldsymbol{n}_{\boldsymbol{k}} \cdot [\boldsymbol{n}_{\boldsymbol{B}} \times \nabla T], \end{aligned}$$

where the coefficient a defined in Eq. (9) is small, $a \ll 1$. Using Eqs. (24) we find the r.h.s of Eq. (10) in the main text,

$$\begin{aligned} &\sum_q (W_{\boldsymbol{q}\to\boldsymbol{k}} f_{\boldsymbol{q}} - W_{\boldsymbol{k}\to\boldsymbol{q}} f_{\boldsymbol{k}}) \qquad (25) \\ &= -\frac{\tau_\omega^{-1}}{4\pi}\sum_{\boldsymbol{q}} \left\{ A^S \boldsymbol{n}_{\boldsymbol{k}} \cdot \nabla T + A^A \boldsymbol{n}_{\boldsymbol{k}} \cdot [\boldsymbol{n}_{\boldsymbol{B}} \times \nabla T] \right. \\ &\left. + a \cdot A^S (\boldsymbol{n}_B \cdot [\boldsymbol{n}_q \times \boldsymbol{n}_k])(\boldsymbol{n}_{\boldsymbol{q}} \cdot \nabla T) \right\} \\ &= -\tau_\omega^{-1}\left\{ A^S \boldsymbol{n}_{\boldsymbol{k}} \cdot \nabla T + (A^A + \frac{a}{3}A^S)\boldsymbol{n}_{\boldsymbol{k}} \cdot [\boldsymbol{n}_{\boldsymbol{B}} \times \nabla T] \right\}, \end{aligned}$$

When calculating (25) we neglect terms $\propto a^2$ and keep in mind that

$$\begin{aligned} \int d\Omega_{\boldsymbol{q}} 1 &= 4\pi \\ \int d\Omega_{\boldsymbol{q}} n_{\boldsymbol{q}\mu} n_{\boldsymbol{q}\nu} &= \frac{4\pi}{3}\delta_{\mu\nu} \ , \qquad (26) \end{aligned}$$

where μ and ν are Cartesian indexes and Ω_q is solid angle. Comparing (25) with l.h.s of Eq. (10) we find the textbook expression for A^S and, we also find the condition $A^A = -(a/3)A^S$. Hence we come to Eq. (12)

$$\begin{aligned} g_k^{(S)} + g_k^{(A)} &= A^S\left(\boldsymbol{n}_{\boldsymbol{k}} \cdot \nabla T - \frac{a}{3}\boldsymbol{n}_{\boldsymbol{k}} \cdot [\boldsymbol{n}_{\boldsymbol{B}} \times \nabla T]\right) \\ A^S &= -\frac{e^{\omega_k/T}}{(e^{\omega_k/T}-1)^2}\frac{c^2}{T^2}\tau_\omega k \ . \end{aligned}$$

[1] C. Strohm, G. L. J. A. Rikken, and P. Wyder, Phys. Rev. Lett. **95**, 155901 (2005).

[2] A. V. Inyushkin and A. N. Taldenkov, JETP Lett. **86**, 379 (2007).

[3] Band gaps in garnets are about 5 eV, see e.g. D. J. Robbins, B. Cockayne, B. Lent, J. L. Glasper, Sol State Commu. **36**, 691 (1980).

[4] J. Hammann and M. Ocio, J. Phys. (Paris) **38**, 463 (1977).

[5] Y. Onose, Y. Shiomi, and Y. Tokura, Phys. Rev. Lett. **100**, 016601 (2008).

[6] H. Katsura, N. Nagaosa, and P. A. Lee, Phys. Rev. Lett. **104**, 066403 (2010).

[7] Y. Onose, T. Ideue, H. Katsura, Y. Shiomi, N. Nagaosa, and Y. Tokura, Science **329**, 297 (2010).

[8] R. Matsumoto and S. Murakami, Phys. Rev. Lett. **106**, 197202 (2011); Phys. Rev. B **84**, 184406 (2011).

[9] M. I. D′yakonov and V. I. Perel′, ZhETF Pis. Red. **13**, 657 (1971) [JETP Lett. **13**, 467 (1971)].

[10] J. E. Hirsch, Phys. Rev. Lett. **83**, 1834 (1999).

[11] For a review, S. Maekawa, *Concepts in Spin Electronics* (Oxford University Press, Oxford, 2006).

[12] L. Sheng, D. N. Sheng, C. S. Ting, Phys. Rev. Lett. **96**, 155901 (2006)

[13] Yu. Kagan and L. A. Maksimov, Phys. Rev. Lett. **100**, 145902 (2008).

[14] L. A. Maksimov and T. V. Khabarova, Doklady Akademii Nauk **442**, 749 (2012) [Doklady Physics **57**, 51 (2012)].

[15] L. Zhang, J. Ren, J.-S. Wang. and B. Li, Phys. Rev. Lett., **105**, 225901 (2010); J. Phys.: Condens. Matter **23**, 305402 (2011). T. Qin, J. Zhou, and J. Shi, Phys. Rev. B **86**, 104305 (2012).

[16] M. Onoda, S. Murakami, and N. Nagaosa, Phys. Rev. Lett. **93**, 083901 (2004).

[17] A. V. Inyushkin and A. N. Taldenkov, JETP Solids and Liquids **138**, 862 (2010).

[18] A. A. Abragam and B. Bleaney, *Electron Paramagnetic Resonance of Transition Ions*. (Clarendon, Oxford, 1970).

[19] P. Fulde, *"Crystal fields", Handbook on the Physics and Chemistry of Rare Earths*, **2**, 295 (1979).

[20] C. Kittel, *Introduction to Solid State Physics*. New York, Wiley, 1966.

[21] J. S. Plant, J. Phys. C: Solid State Phys, **10**, 4805 (1977).

[22] Throughout this paper, we set both Planck's constant and Boltzmann's constant equal to unity: $\hbar = k_B = 1$.

[23] J. A. Koningstein, C. J. Kane-Maguire. Can. J. Chem. **52**, 3445 (1974).

[24] J. Hammann and P. Manneville, J. Phys. (Paris) **34**, 615 (1973).

[25] L. D. Landau and E. M. Lifshitz, Quantum Mechanics Non-Relativistic Theory, Third Edition: Volume 3

[26] N. P. Kolmakova, R. Z. Levitin, A. I. Popov, N. F. Vedernikov, A. K. Zvezdin, and V. Nekvasil, Phys. Rev. B **41**, 6170 (1990).

[27] The $|\pm M\rangle$ states are composed of states with definite z-projection of the ion angular momentum J such as, $|+M\rangle = ...|+2\rangle + \alpha_+|+1\rangle + \alpha_0|0\rangle + \alpha_-|-1\rangle + ...$, and $|-M\rangle = ...|-2\rangle - \alpha_+|-1\rangle + \alpha_0|0\rangle - \alpha_-|+1\rangle + ...$

[28] F.W. Sheard and G.A. Toombs, Solid State Communications **12**, 713 (1973).

[29] G.A. Toombs and F.W. Sheard, J. Phys. C: Solid State Phys. **6**, 1467 (1973).

[30] S. L. Adler, Phys. Rev. **137**, B1022 (1965).

[31] In the skew part we account only for the virtual c-state and neglect the virtual d-state. This is because $\Gamma_{d\omega}/\Omega_{ad}^2 \ll \Gamma_{c\omega}/\Omega_{ac}^2$ and hence the skew component for the d-state is relatively small.

[32] A. Fert, J. Phys. F: Metal Phys. **3**, 2126 (1973).

[33] W. Kohn and J. M. Luttinger, Phys. Rev. **108**, 590 (1957).

[34] R. Berman, *Thermal Conduction in Solids* (Clarendon, Oxford, 1976).

[35] G. L. J. A. Rikken and B. A. van Tiggelen, Nature **381**, 54 (1996).